

Finite-State Machine for Level-Ground Walking Control of an Ankle-Foot Orthosis

Joseph Tsongo Vughuma, Olivier Verlinden,

University of Mons

Boulevard Dolez 31, 7000 Mons/Belgium

Joseph.tsongovughuma@umons.ac.be; Olivier.verlinden@umons.ac.be

Abstract - This paper presents a control algorithm for an active ankle-foot orthosis that provides level-ground walking assistance with adaptable control parameters. Instead of the impedance-control usually used in lower-limb assistive devices, an admittance control is used, and the control parameters are adapted with respect to gait events detected by a finite-state machine based on foot pressure sensors. In this work, the state machine can not only detect the various phases of the walking cycle but also undesirable events such as an unexpected lifting of the foot, reversing or even the user's intent to stop. It selects the best parameters that will allow a safe control of the orthosis. The control system was implemented and evaluated on a single subject. The ability of the device to provide appropriate functionality (kinematics and kinetics) during ground-walking is compared to those of a healthy subject. Results from tests indicates that the orthosis can provide desirable level-ground walking behavior.

Keywords: Control, Ankle, Impedance, Orthosis, Walking, Admittance, Finite-state machine

1. Introduction

Walking is a common activity of daily living yet complex in its mechanism. It involves all levels of the nervous system and many parts of the musculoskeletal apparatus as well as the cardiorespiratory system. A person's gait pattern is strongly influenced by age, personality, and medical condition. In 2017, the number of people in Europe aged 60 years and over exceeded 183 million, with a clear increasing tendency. Furthermore, every year, more than 9 million people suffer from stroke and several other neurological accidents, among which 7 million result in physical disability [1]. Consequently, walking capability can be affected in these groups of people because safe walking requires intact cognition and executive control. Some of them show gait pathologies that can threaten their safety and their autonomy [2-3]. The source of gait pathologies is impairment of limbs and their joints. A special attention will be paid to the foot-ankle joint in our work.

Technological advancements have led to the development of numerous wearable microprocessor-controlled robotic devices that are mechanically powered for the assistance of the ankle and restoration of human locomotion [4-8]. These devices use a variety of control strategies such as impedance/admittance-based control model [9-10], trajectory tracking [11-12], artificial reflexes, or musculoskeletal model [6]. In general, a control strategy has a 3-level hierarchical structure [13]. The first level (high level) is a perception level where the controller must perceive the user intents or identify the task such as standing, level walking or ascending/ descending stairs. The second level (mid-state) translates the first level detected intention or task into a device state (gait phases related to the task) then select adequate parameters which are used by the low-level control (controller: third level (low level)) to send commands to the actuator(s). This means, regardless of the low-level control implemented for a device, a mid- or/and high-level control is/are used in combination. The most used by peers is the finite state machine (FSM) ([4][6][11] [14-15]). It has a central role in the first decisions making considering the interaction between the controller, the user, the environment, and the mechanical device itself [13]. As said, FSM not only enables the new generations of orthosis / prosthesis to detect switch between ground walking, ascending, and descending stairs, or ascending and descending ramp mode, but also to detect the different gait phases of the aforementioned activities to assist the user as needed.

The implementation of FSM relies on information coming from sensors located all around the device. Various finite state machines exist and have been presented and commented by several authors. The most common algorithms are based on electromyography (EMG) [4-5][16], gyroscope/accelerometers (IMU) [17-18] and pressure sensors [19].

FSMs work well for gait detection no matter the technology behind. But they are principally designed for forward progression of the user. Few have developed or commented the capability of their FSMs to manage backward progression [5] or unpredictable movements [4][5]. For the most part, this information is not given, or the topic is not developed explicitly.

Since these orthotic/prosthetic (P/O) devices evolve toward daily use, it is important to manage every single situation that can happen while ensuring that the control for forward progression remains effective.

The goal of this work is to propose, for an active ankle-foot orthosis, an efficient control strategy which relies on a robust finite-state machine, combined with an adaptable admittance control to assist dorsiflexion and plantarflexion (full gait cycle) for level ground walking. The admittance control allows to emulate electronically the compliant behavior of a Series Elastic Actuator (SEA). It confers a great flexibility because the stiffness is just a parameter of the controller and can be changed within the algorithm. The FSM detects gait phases and gait abnormalities and depending on the detected events selects adequate parameters for the main controller which ensures the safety of the user and optimal control of the device.

2. Material and Control Target

2.1. Material

The system studied was described in [20]. The orthosis shell is in titanium and the foot support is in Ultem reinforced with carbon fibers. It was designed by 3D scanning the foot and shank of a patient. The actuator is fully self-assembled at the Department of Theoretical Mechanics, Dynamics, and Vibration of the University of Mons. It is composed of a brushless motor with coreless rotor combined with a roller screw drive which converts the rotation of the motor in linear displacement which is further converted in rotation of the foot support. The motor is equipped with Hall Effect sensors for commutation and optical encoder for position information. A PIC32 microcontroller receives signals coming from motor encoder, load sensor (attached at the end of the roller screw) and pressure sensor. Two pressure sensors are used for the finite-state machine. One is located at the heel and the other at the forefoot. A driver is added to control the brushless motor.

2.2. Gait cycle description

Research on the ankle-foot biomechanics during level-ground walking has led to the division of the gait into two main phases [21][22]: the stance phase when the foot is in contact with the ground (60 % of a gait cycle) and the swing phase (SW) when the foot is off the ground (TO) (40 % of a cycle) (Fig. 1).

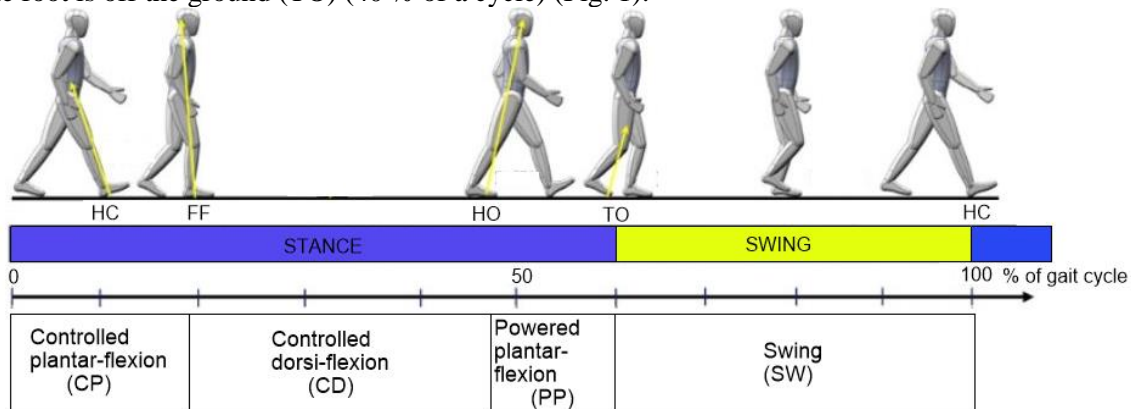


Fig. 1: Gait cycle.

Biomechanically speaking, the stance phase can further be divided into three sub-phases:

- Controlled Plantar Flexion (CP): begins at the strike of the heel (Heel contact: HC) on the ground and ends at the contact of the forefoot with the ground (Foot-flat: FF). The ankle behaves like a linear spring. It is illustrated by the segment HC-FF in Fig. 2 which represents the evolution of the ankle torque versus the ankle angle.

- Controlled Dorsiflexion (CD): begins when both the forefoot and heel are in contact with the ground (FF) and continues until dorsiflexion reaches a maximum point, when the heel lifts off the ground (HO). The ankle behaves like a non-linear spring with energy storage (FF-HO in Fig. 2). This energy will be released in the following phase and will help to propel the body forward.
- Powered Plantarflexion (PP): it begins when the heel leaves the ground (HO) and ends at Toe-off (TO). At the beginning of powered plantarflexion, the energy stored by the non-linear spring is released to lift off the foot and propel the body. In general, the energy released by the spring is not enough. Therefore, additional energy is provided by the ankle besides the energy stored previously.

The dynamics of an ankle during a gait cycle results in a curve shaped like the one presented in Fig.2 (curve for an 80 kg male human walking at 1.25 m/s [23]). The inner surface of the curve is the image of the net energy produced by the ankle.

An active ankle-foot orthosis/prosthesis must be able to reproduce this spring-like behavior.

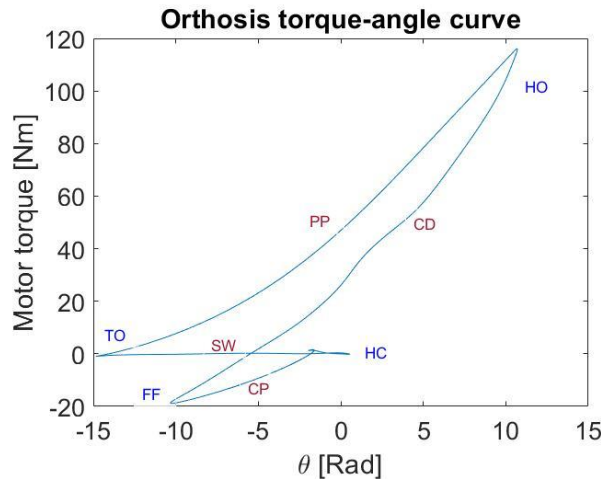


Fig. 2: Torque-angle curve.

2.3. Control method

Before defining the control target, it can be interesting to analyze the dynamics of the ankle. A dynamics equilibrium at ankle joint (Fig. 3) when the foot is on the ground can be made:

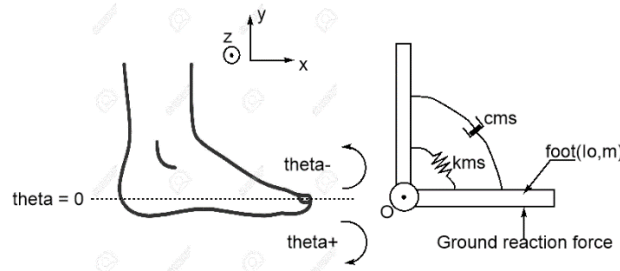


Fig. 3: Ankle model.

$$-I_O \ddot{\theta} - c_{ms} \dot{\theta} - k_{ms}(\theta - \theta_0) - T_g + T_{grf} = 0 \quad (1)$$

I_O is the moment of inertia of the foot with respect to the ankle axis, k_{ms} and c_{ms} the equivalent stiffness and damping of the musculoskeletal system acting on the ankle respectively, T_g gravity torque related to the weight of the foot, T_{grf} the ground reaction torque and θ the ankle rotation (the zero reference of the ankle rotation is the perpendicular to the leg). In prostheses devices, the biological ankle-foot joint complex is replaced by the ankle prosthesis which has a lightweight foot. The necessary torque, to replicate the behavior of the biological ankle, is provided by the prosthesis motor. Thus, the equation (1) can be reduced to:

$$T_m = -T_{grf} \quad (2)$$

k_{ms} and c_{ms} are equal to zero and, thanks to the lightweight foot, I_O and T_g are negligible. T_m is the device torque.

In orthosis devices since the biological ankle-foot joint complex still exists and must be included in the development. The device goal is to provide the additional torque to compensate/assist the impairment. All torques in equation (1) must be considered and the motor torque, T_m is added:

$$-I_O\ddot{\theta} - c_{ms}\dot{\theta} - k_{ms}(\theta - \theta_0) - T_g + T_{grf} + T_m = 0 \quad (3)$$

However, some components of equation (3) can be neglected.

On average, the value of the moment of inertia I_O of the foot is 0.02 kgm^2 [24][25]. The maximal acceleration occurs at the propulsive phase. In moderate walking speed ($0.4\text{-}1.20 \text{ m/s}$), the value of maximal acceleration is 91 rad/s^2 [5][26]. This implies that the inertial torque is max 1.82 Nm .

In our work, the orthosis is designed for a patient with a neuromuscular problem which does not allow him to produce any active musculoskeletal torque at the ankle. However, passive action of muscles and tendons remains. [27] and [24] analyzed the passive stiffness and damping of patient with similar neuromuscular problem resulting from stroke. The overall k_{ms} and c_{ms} were respectively equal to $47.9 \pm 11.82 \text{ Nm/rad}$ (dorsiflexion) and 1.5 Nms/rad . The maximum dorsiflexion occurs just before the propulsive phase and if the maximal speed occurs at the same time (4 rad/s [26]) the resulting torque is 17 Nm (max speed = 4 rad/s , max dorsiflexion angle 15°). The maximum inertia + passive musculoskeletal torque is equal to 18.82 Nm , which corresponds to 15% of the maximal torque T_{grf} presented in Fig. 2.

That, equation (2) can be also used, for an active orthosis. This also means that the orthosis must replicate the torque-angle curve in Fig. 2.

The control target is then defined as shown in Fig. 4 [20,4]: the curve can be replicated by using two linear springs with different stiffness k_{hs} , k_{ff} and a torque source that provides positive net work during the powered plantarflexion. Each stiffness corresponds to the slope of the curve and the additional torque is provided by changing the spring rest angle θ_0 , denoted by p_0 (0° by default), p_1 and p_2 . The control target was first explained in [20]. p_1 provides the propulsive torque and p_2 is the change in the rest angle to maintain torque continuity when changing the stiffness at 0 rad . Fig. 4 represents the control target. Only 4 parameters are necessary to completely reproduce the angle/torque curve. This curve differs from one individual to another, consequently those 4 parameters will differ from one user to another and should be chosen wisely.

The advantage offered by the control is the flexibility of the algorithm due to the fact that the adaptation of one individual to another is only due to the change of those 4 parameters in the control algorithm.

3. Control implementation

In the previous section, the control target was presented. The control must reproduce the compliant behavior of a spring whose stiffness and equilibrium position change over the cycle. The changes occur after specific event (HC, FF, HO, TO),

therefore those events need to be detected first. This is done by using a finite-state machine. The latter will be introduced later.

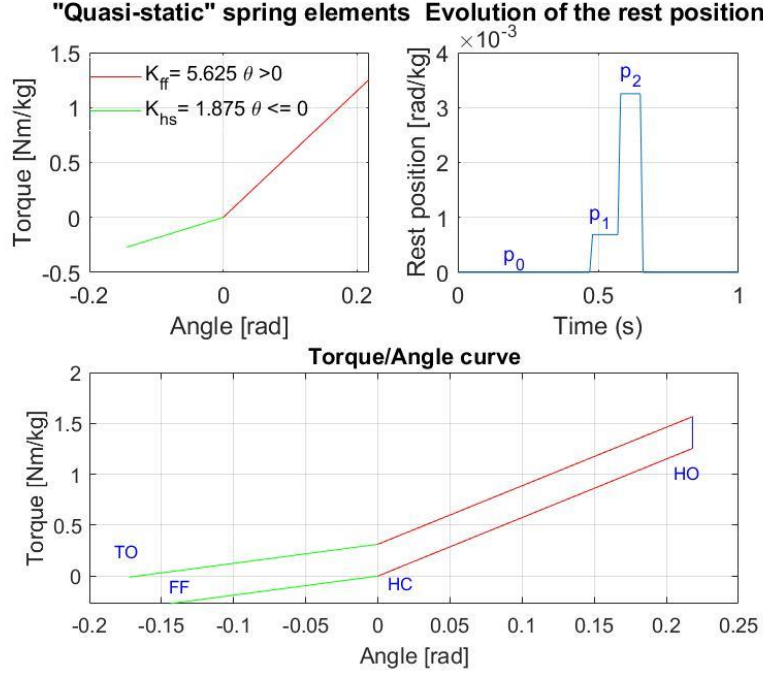


Fig. 4: Control target.

3.1. Admittance control

The active compliant control is divided to two types of control, admittance control and impedance control. The admittance control scheme uses an inner position loop and an outer force/torque loop, while the impedance scheme does the opposite. In both cases the desired impedance/admittance is implemented in the outer loop while the inner closed loop is supposed to be fast enough so that its dynamics can be neglected [28]. To replicate the compliant behavior of the ankle presented in the previous section, several authors used a SEA combined with an impedance-based control of the motor [29]. In such control, the torque is calculated as:

$$T_m = k_i(\theta_a - \theta_{0i}) + b_i \dot{\theta}_a \quad (4)$$

Where T_m , θ_a and $\dot{\theta}_a$ denote ankle torque, ankle angular position, and ankle angular velocity of the device, and k_i , b_i and θ_{0i} the stiffness, damping coefficient, and equilibrium angle for the i^{th} state detected by the finite-state machine. Due to the lack of physical spring in our device, the common impedance control cannot be implemented. Consequently, an admittance control of the motor is performed. Fig. 5 shows a diagram of an admittance control. The classical position loop control is combined with a second loop coming from the sensed force/torque at the end of the motor. The second loop control deals with the sensed force/torque exerted on/by the motor. It is divided by the desired stiffness to obtain a displacement which is the equivalent of the displacement that would have a physical spring in presence of the same torque.

$$\theta_{\text{setpoint}}(s) = T(s)A(s) + \theta_{0i}(s) \quad (5)$$

$$\theta_{\text{setpoint}} = T/K_i + \theta_{0i} \quad (6)$$

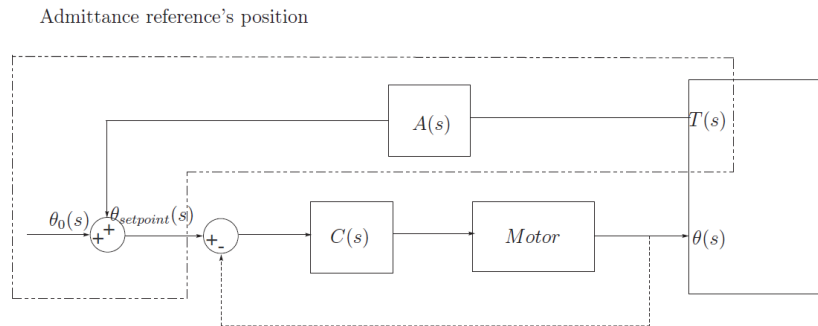


Fig. 5: Caption for figure goes at the bottom.

With $A(s) = 1/K_i(s)$, $T(s)$ sensed force/torque, $\theta_{0i}(s)$ the rest position, $\theta(s)$ the angular position of the orthosis, $C(s)$ the position controller and K_i the desired stiffness.

3.2. Finite-state machine

A gait cycle is divided in several phases and subphases and the stiffness and rest angle of the orthosis change from one phase to another. To perform an efficient control, it is necessary to detect the different phases so the control parameters can be changed accordingly. This is done by means of a finite-state machine. The finite state machine has two purposes here: first to detect gait phases, then to select correct parameters to send to the compliant controller.

The transition from one state to another is done by the detection of events. To detect those events, two sole pressure sensors, one placed at the heel and the other at the forefoot are used. The state of a sensor will be considered as active “1” when the pressure measured is above a chosen threshold and inactive “0” when it is below the threshold. The state is "active" means that, the contact with the ground is effective and "inactive" otherwise.

Remark: 00,10,01,11 express the states of the pressure sensors, with the first digit referring to the heel and the second to the forefoot.

During a standard forward gait, the states and their transitions can be seen as following (Fig. 6.a).

Init (0): This is the state at power on (device initialization). This state remains active until only the foot-flat event (11) is detected (the detection of the foot-flat will be considered as the sign that the user wants to initiate the gait). For this particular state, the forefoot sensor threshold is put at a higher value than normal to ensure that the body mass transfer is correctly done to initiate the gait.

Init (0) → foot-flat: When both the heel and the forefoot sensors are active “11”, the foot-flat event is detected, and state (1) is activated. This phase corresponds to the **controlled-dorsiflexion (CD (1))** (Fig. 1 and 2: FF-HO).

Foot-flat → Heel-off: if the heel sensor is deactivated and the forefoot sensor remains active “01”, the heel-off event is detected and state (2) is activated. This phase corresponds to the **powered-plantarflexion (PP (2))** (HO-TO).

Heel-off → Toe-off: In PP (2) when both sensors become inactive “00”, the toe-off event is detected, and a new state (3) is activated. Here there is no more contact of the foot with the ground. State (3) is the **swing phase (SW (3))** (TO-HC).

Toe-off (3) → heel-strike (4): from the SW(3) when the heel enters in contact with the ground the heel-strike is detected, and a new state (4) is activated. This phase corresponds to the **controlled-plantarflexion (CP (4))** (HC-FF).

Heel-strike (4) → foot-flat (1): In this state, when the forefoot sensor activation is detected both the heel and forefoot sensors are active (11) thus CD is active (1) (FF-HO).

These 4 states (+Init) cover the entire gait cycle. However, unexpected moves can happen forcing the user to move backward, for example. The state machine must manage these transitions to allow the controller to act safely. Also from each state, there are four possible combinations of the transition. For example, in PP (2) “01”, you can either move forward to SW

(3) “00” or moving backward to CD (1) “11” or stay in PP (2) “01” or see the sensors going from “01” to “10”. Therefore, for every state, all the possible transitions must be managed (Fig. 6.b).

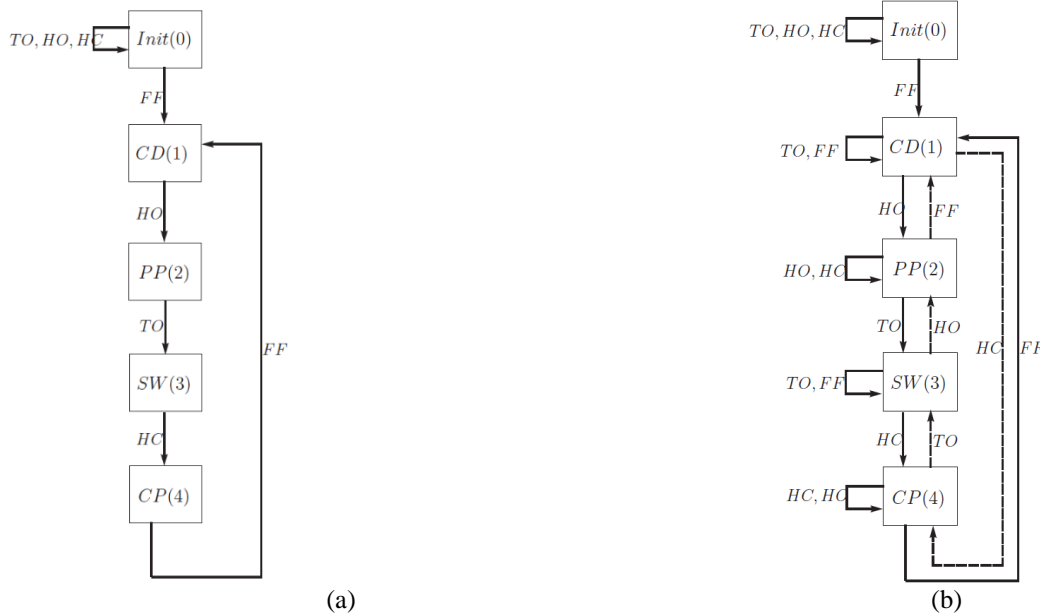


Fig. 6: Basic finite-state machine 1(a) and 2(b).

The representation in Fig. 6.b is still not complete. Indeed, in PP if the sensor states change to (10), the CP (4) “10” should be reached. However, going to CP (4) from PP (2) is not a normal move because the "normal" way to transition to that state is by coming from SW (3) (forward) or CD (1) (backward). Therefore, a new state is created, state 6 (**Controlled-dorsiflexion safety (CDS)**), which indicates that SW (3) was expected but CP (4) was detected instead. It has the same sensor states as CP (4) but transition was bad (Fig. 7.a). This can indicate a problem in the walking process.

The same reasoning must be applied to every state. Thus, a more complex structure must be implemented. There are principally two advantages of creating new states: first it will allow to detect unexpected transitions while ensuring the gait phases are still detected. Secondly, it will prevent injuries by putting the system in safety state.

The backward movement is just the opposite of the forward movement ($1 \rightarrow 2 \rightarrow 3 \rightarrow 4$ for forward and $4 \rightarrow 3 \rightarrow 2 \rightarrow 1$ for backward) and can easily be detected by the FSM. From the control point of view, there could be a problem, when moving backward since the ankle does not act the same for the two directions, especially when energy should be delivered by the orthosis (propulsion). Therefore safety states have to be created.

The structure in Fig. 7.b presents a more complete finite-state machine. With addition of safe state deriving from normal state (CD (1), PP (2), SW (3) and CP (4)) to protect the user from injuries. Time limit T_{max} and T_{max2} are also added to not spend too much time in certain sensible state, particularly PP (2) where the propulsion is generated.

3.3. Finite-state machine + admittance control

The purpose of a state machine, regardless of the technology used, is to be able to detect user intentions and act on the controller accordingly. Every state reached by the FSM selects specific control parameters as presented in Table 1. These parameters are chosen to match the control target defined in section 2.3, Fig. 4.

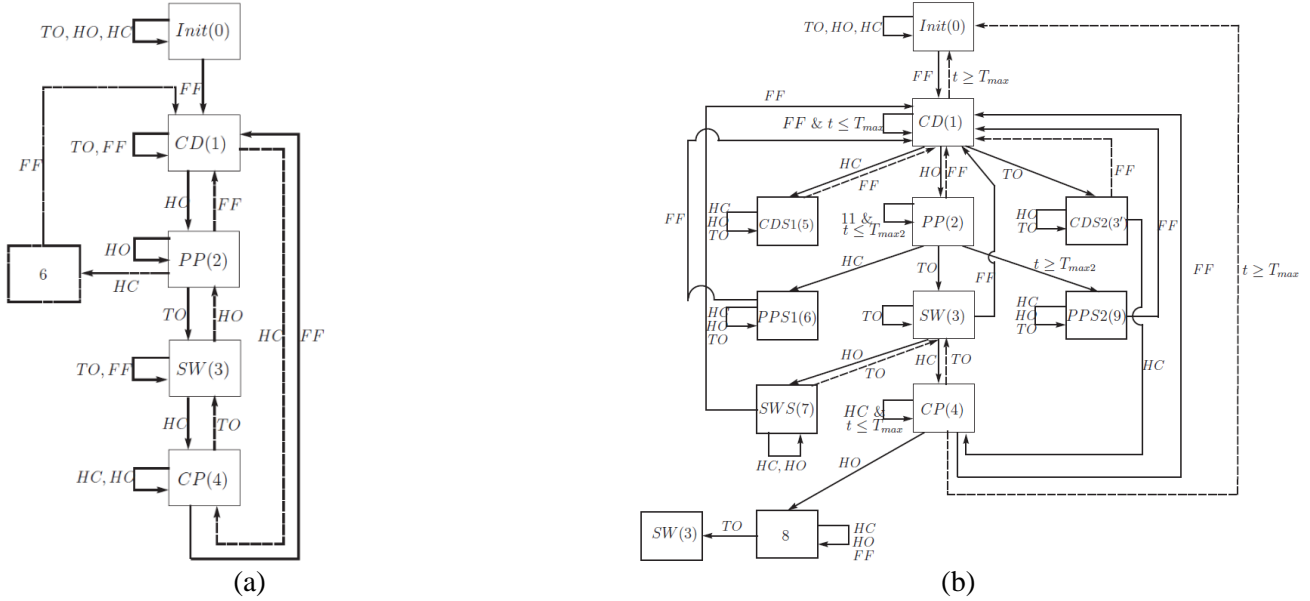


Fig. 7: Basic finite-state machine (a) and final finite-state machine (b).

Table 1: Control parameters selection.

State	Angular stiffness	Rest angle x_0
<i>Init (0)</i>	k_{ff}	p_0
<i>FF (1)</i>	If $\theta \geq 0$	k_{hs}
	If $\theta < 0$	k_{ff}
<i>PSW (2)</i>	If $\theta \geq 0$	p_1
	If $\theta < 0$	p_2
<i>SW (3)</i>	-	p_0
<i>HC (4)</i>	k_{hs}	p_0
<i>All Safety Sates</i>	k_{ff}	p_0

With θ the angular displacement of the orthosis.

4. Implementation

4.1. Finite-state machine

- Sensors signals are smoothed using a digital filter. This action introduced a delay of 5 microseconds.
- A Bluetooth module sends the various data captured and calculated to a computer to store and analyze them.

4.2. Controller

- The controller has been implemented in the microcontroller. The control loop runs at 500 Hz.
- The signal from the force sensor is also smoothed by a digital filter introducing a 5 microseconds delay. A calibration of the force sensor was made as recommended by the supplier
- An encoder read the motor position (converted in angular position). This position is used in the feedback loop of the admittance controller and converted to speed by the amplifier for speed control.

5. Single subject experiment

5.1. Setup

The tests were carried out on 6 different days: March 11, 13 and 16, April 28 and December 17 and 18 2020, on a single subject of 1.78m, 92kg, 27 years old with still functional ankle. The electronics of the orthosis were placed in a backpack worn by the subject. The orthosis was rigidly attached to the foot and the shank of the subject using solid knots (Fig. 8). The subject stood behind a drawn line, the finger on an initialization switch. When ready, he could release the switch and wait 5 seconds (the time it takes for the orthosis to initialize) and then start walking at a self-selected speed. He walked in a straight line for about 11 meters. The most important and most complicated task for the subject was to soften the ankle so that active muscles did not act on the ankle.

A 3rd pressure sensor was placed below the foot at the toe level to measure the real contact force between the orthosis and the ground (the **ground reaction force** (converted in **ground reaction torque GRT**)).

Parameters used for the admittance controller:

- $k_{hs} = 200 \text{ Nm/rad}$
- $k_{ff} = 450 \text{ Nm/rad}$
- $p_0 = 0 \text{ rad}$
- $p_1 = 0.49 \text{ rad}$
- $p_2 = 0.84 \text{ rad}$
- Position control (P-I): $K_{pp} = 31.5 \text{ s}^{-1}$, $K_{ip} = 164.35 \text{ s}^{-2}$.
- Speed control Accelus (P-I): $K_{pv} = 800 \text{ A/rad/s}$, $K_{iv} = 25 \text{ A/rad}$



Fig. 8: Subject's foot.

5.2. Results and discussion

Fig. 19.a shows a randomly chosen result. It represents the torque/angle curve of the orthosis for one cycle of walking. The curve agrees with literature curves (Fig. 2). The stiffnesses implemented are well respected by the compliance control. The surface created by this curve represents the work done by the orthosis, which is a consequence of the production of the propulsive torque during the push-off phase (powered plantarflexion-state PP (2)). It is about 10.45J.

In Fig. 9.b, three curves are compared. The torque produced by the orthosis, which is supposed to be equal to the ground reaction torque (equation (2)), the measured ground reaction torque and the ground reaction torque generated by a healthy ankle.

we can see that the orthosis torque and the measured ground reaction have the expected curve profile. However, the maximum torque produced by the ankle for a moderate walking speed is expected to be higher than what was measured (98kg the weight of the subject), but it is not. This difference can be a consequence of either the passive musculoskeletal system torque of the ankle or additional torque due to the active muscles that intervened when walking. The second hypothesis seems to be the most probable.

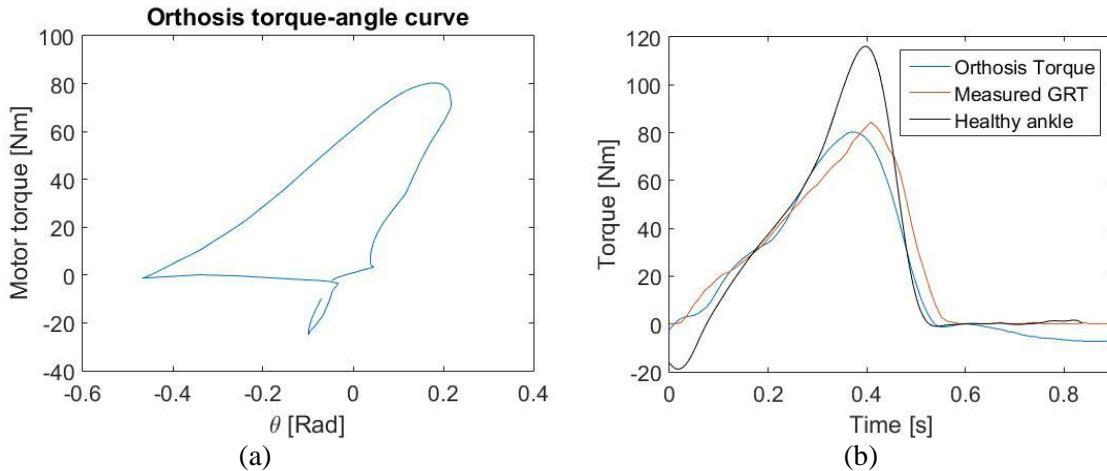


Fig. 9: Measured torque/angle curve of the orthosis for one cycle of walking (a) and Torque/time curves comparison (b).

In future works, when working with a non-impaired subject, it would be interesting to measure the activity of the muscles during the test to correctly customize the parameters of the controller to have better assistance of the ankle.

As depicted in Fig. 10, the healthy ankle angle cycles between approximately 15° of dorsiflexion (before the push-off) and 20° of plantarflexion (end of push-off). The active orthosis similarly cycles between these configurations. The overall profiles show a good agreement between the orthosis and healthy subject.

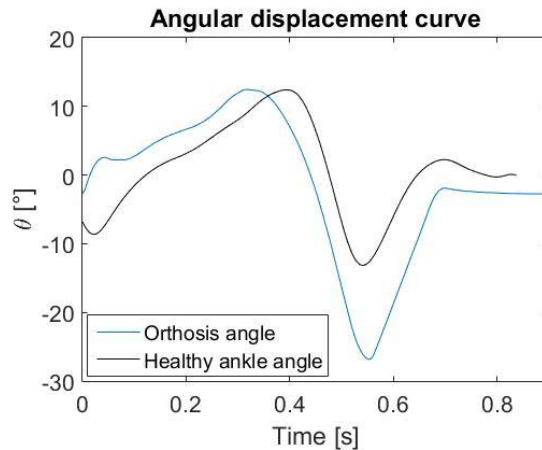


Fig. 10: Measured angle curve (Orthosis angle) and literature ankle angle profile (Healthy ankle angle).

On the other hand, the success of the control also implies that the phase detection is functioning properly. For the sake of illustration, Fig. 11 shows the detection made by the FSM for an operating cycle related to the result in Fig. 9.

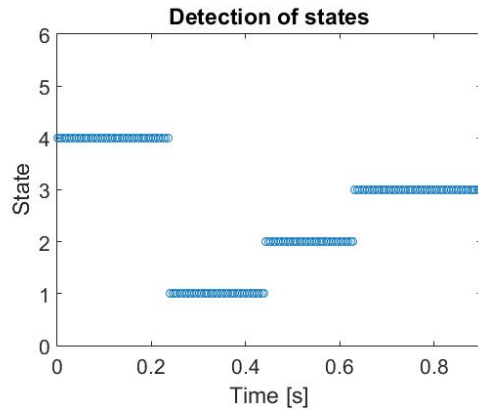


Fig. 11: FSM State detection.

Fig. 12.a is a sample of the results obtained during the tests. It presents the evolution of states over several walking cycles (over the 11 meters). Fig. 12.b details the 5th cycle thereof, showing a 60-40% ratio between the stance and the swing phases as in literature

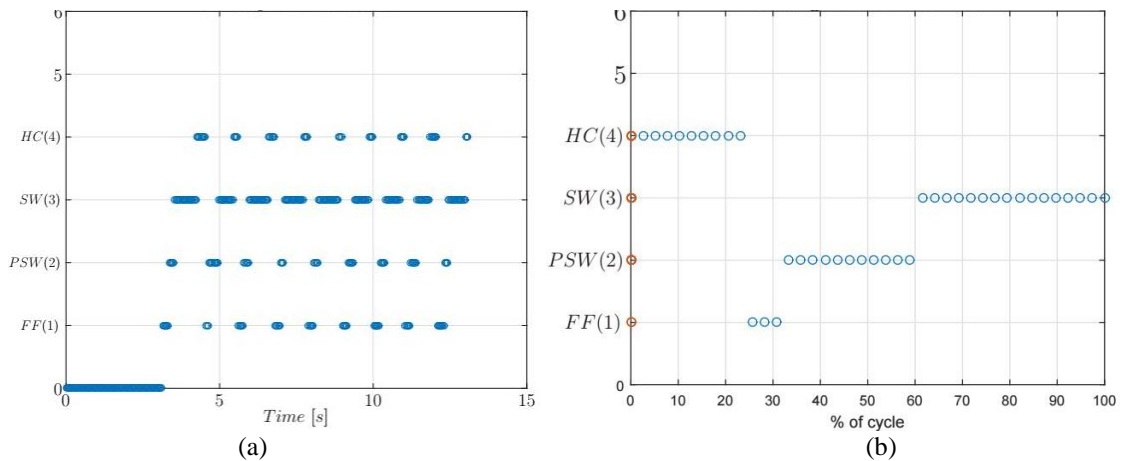


Fig. 12: FSM state detection over several cycle (a) and FSM state detection for one cycle (b).

During the tests the "safety" states were reached rarely (an example in Fig. 13.b state 5) but the FSM comes back naturally to normal states. The consequence of safe state in the control is that the orthosis, to be safe for the user, act like a passive orthosis (Fig. 13.a).

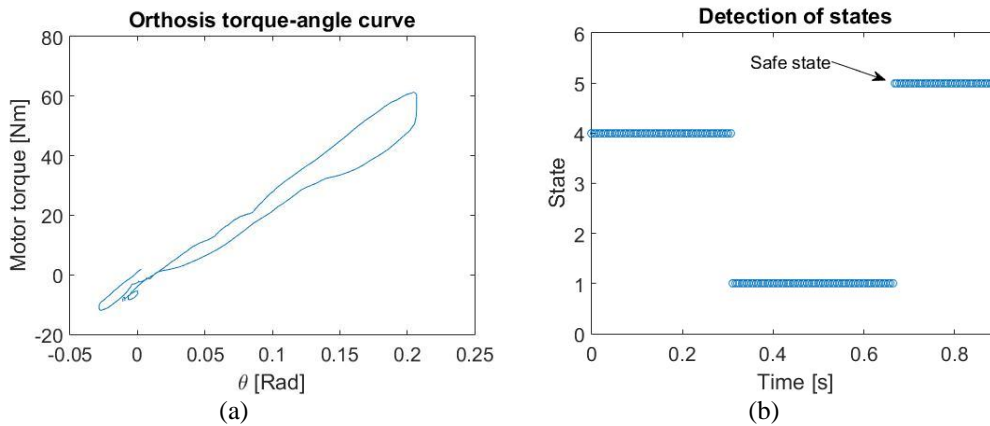


Fig. 13: Measured torque/angle curve of the orthosis for one cycle of walking (a) and corresponding FSM detection (b).

6. Conclusion

A level-ground walking controller for an active ankle prosthesis was described in this paper. Tests were carried out on a single not impaired volunteer (6 test campaigns) and were satisfactory. Indeed, the orthosis and the controller have managed to reproduce properly the torque/angle evolution observed on a healthy subject. The implemented stiffnesses are well respected and the system provides propulsion (energy production) resulting in positive work of 10.45J.

The admittance control offers great flexibility to the control system. Indeed, given that the parameters can be changed within the algorithm itself, adapting the system from one patient to another implies only changing 4 parameters k_{ff} , k_{hs} , p_1 and p_2 . These parameters must be chosen carefully not only to ensure patient comfort and safety but also ensure to provide the necessary propulsive energy to move forward. Literature provides reference values for k_{ff} and k_{hs} .

The control structure also provided a good robustness thanks to the efficient and reliable finite-state machine (FSM). The proposed FSM does not only detect normal gait phase but also unexpected transition that can happen during forward walking such as moving backward etc... It managed to have correct transitions (moving forward) with a reliability of 93%, which led to correct selection of control parameters. For the 7% reminding, the safe-mode parameters were selected to ensure the passive behavior of the ankle by selecting a low stiffness.

However, the orthosis has shown its sensitivity to musculoskeletal torque. It can be interesting for future work, if tests are done again on a subject with healthy ankle, to measure the active muscle torque to correctly evaluate its influence. But as the orthosis is intended to be used on a patient whose ankle muscles do not work, what can be interesting is to evaluate the real passive stiffness and damping exhibited by the ankle.

For future work, we intend to develop a technique to automatically find the 4 control parameters to be used on a patient and automatically upgrade them while walking.

References

- [1] H. A. Wafa, C. D. Wolfe, E. Emmett, G. A. Roth, C. O. Johnson, and Y. Wang, "Thirty-year projections of incidence, prevalence, deaths, and disability-adjusted life years," *Stroke*, vol. 3, p. 2418–2427, 2020
- [2] W. Pirker and R. Katzenschlager, "Gait disorders in adults and the elderly," *Wiener klinische Wochenschrift*, p. 81–95, 2007
- [3] P. G. Adamczyk and A. D. Kuo, "Mechanisms of Gait Asymmetry Due to Push-Off Deficiency in Unilateral Amputees," in *IEEE Transactions on Neural Systems and Rehabilitation Engineering*, vol. 23, no. 5, pp. 776–785, Sept. 2015
- [4] J. Blaya and H. Herr, "Adaptive control of a variable-impedance ankle-foot orthosis to assist drop-foot gait," *IEEE Transactions on Neural Systems Rehabilitation engineering*, vol. 12, pp. 24–31, 2004.
- [5] M. Holgate, A. Bohler, and T. Suga, "Control algorithms for ankle robots: A reflection on the state-of-the-art and presentation of two novel algorithm," *IEEE RASEMBS International Conference on Biomedical Robotics and Biomechatronics*, vol. 2, p. 97–102, 2008

- [6] Eilenberg MF, Geyer H, Herr H. "Control of a powered ankle-foot prosthesis based on a neuromuscular model". *IEEE Trans Neural Syst Rehabil Eng*. 2010 Apr;18(2):164-73
- [7] Bergelin, B. J., and Voglewede, P. A. (May 2, 2012). "Design of an Active Ankle-Foot Prosthesis Utilizing a Four-Bar Mechanism." *ASME. J. Mech. Des.* June 2012
- [8] R. D. Bellman, M. A. Holgate, and T. G. Sugar, "SPARKy 3: Design of an active robotic ankle prosthesis with two actuated degrees of freedom using regenerative kinetics," *2nd IEEE RAS & EMBS International Conference on Biomedical Robotics and Biomechatronics*, 2008, pp. 511-516
- [9] Anil Kumar, Namita & Hong, Woolim & Hur, Pilwon. "Impedance Control of a Transfemoral Prosthesis using Continuously Varying Ankle Impedances and Multiple Equilibria". *IEEE Int Conf Robot Autom.* (2020).
- [10] Krishan Bhakta, MS, Jonathan Camargo, MS, Pratik Kunapuli, BS, Lee Childers, PhD, CP, Aaron Young, PhD," Impedance Control Strategies for Enhancing Sloped and Level Walking Capabilities for Individuals with Transfemoral Amputation Using a Powered Multi-Joint Prosthesis", *Military Medicine*, Volume 185, Issue Supplement_1, January-February 2020, Pages 490–499
- [11] Zuo Q, Zhao J, Mei X, Yi F, Hu G. "Design and Trajectory Tracking Control of a Magnetorheological Prosthetic Knee Joint". *Applied Sciences*. 2021
- [12] Serrano, Hugo & Luviano-Juárez, Alberto & Chairez, Isaac. "Robust Control of Semi-active Ankle Prosthesis Driven by Electromyographic and Electro-goniometric Signals". *IFMBE Proceedings*. 49. 277-280. 2015.
- [13] Tucker M.R., Olivier J., Pagel A., Bleuler H., Bourri M., Lamercy O, J del R Millán, Riener R., Vallery H., Gassert R.. "Control strategies for active lower extremity prosthetics and orthotics: a review". *J NeuroEngineering Rehabil* 12, 1 (2015).
- [14] Frank Sup, Varol HA., Goldfarb M, "Upslope walking with a powered knee and ankle prosthesis: Initial results with an amputee subject". *Neural Syst Rehabil Eng IEEE Trans* 2011;19(1):71–78.
- [15] Goršič M, Kamnik R, Ambrožič L, Vitiello N, Lefeber D, Pasquini G, Munih M. "Online phase detection using wearable sensors for walking with a robotic prosthesis". *Sensors* 2014;14(2):2776–94.
- [16] Ferris D., Gordon K., Sawicki G., and Peethambaran A, "An improved powered ankle-foot orthosis using proportional myoelectric control," *Gait posture*, vol. 23, pp. 425–428, 2006.
- [17] Zhao H, Zhelong W, Sen Q, Jiabin W, Fang X, Zhengyu W, Yanming S, "Adaptive gait detection based on foot-mounted inertial sensors and multi-sensor fusion", *Information Fusion*, Volume 52, 2019, Pages 157-166
- [18] De Coeyer, Dylan ; Legrand, Alicia. "Adaptive control of an active ankle prosthesis". *Ecole polytechnique de Louvain, Université catholique de Louvain*, 2020. Prom. : Ronsse, Renaud
- [19] D. De Wit, J. Buurke, J. Nijlant, M. Ijzerman, and H. Hermen, "The effect of an ankle-foot orthosis on walking ability in chronic stroke patients: a randomized controlled trial." *Clinical Rehabilitation*, vol. 18, p. 550–557, 2004
- [20] J. Tsongo Vughuma and O. Verlinden, "Control algorithm for an active ankle-foot orthosis(aafos): Adaptive admittance control," *ICBBE 19: 2019 6th International Conference on Biomedical and Bioinformatics Engineering*, 2019
- [21] Samuel K Au, Herr H, Weber J, Martinez-Villalpando E.C, "Powered ankle-foot prosthesis for the improvement of amputee walking economy," *PhD thesis, Department of Mechanical Engineering, MIT*, 2007.
- [22] R. Neptune, S. Kautz, and F. Zajac, "Contributions of the individual ankle plantar flexors to support, forward progression and swing initiation during walking," *Journal of biomechanics*, vol. 34, pp. 1387–1398, 2001.
- [23] Holgate M, Hitt J.K, Bellman R.D, Sugar T.G, Hollander K.W, "The sparky (Spring Ankle with Regenerative Kinetics) Project: Choosing a DC Motor Based Actuation Method", *Conference on Biomedical Robotics and Biomechatronics*, 2008.
- [24] M. Mirbageri, H. Barbeau, M. Ladouceur, and R. E. Kearney, "Intrinsic and reflex stiffness in normal and spastic, spinal cord injured subjects," *Experimental Brain Research*, vol. 141, p. 446–459, 2001.
- [25] Veneva I, "Intelligent device for control of active ankle-foot orthosis," *International conference in biomedical engineering*, 2010.

- [26] B. Mentiplay, M. Banky, R. Clark, M. Kahn, and G. Williams, "Lower limb angular velocity during walking at various speeds," *Gait Posture*, vol. 65, pp. 190–196, 2018
- [27] Roy A, Krebs H.I, Patterson S.L, Judkins T.N, Khanna I, Forrester L.W, Macko R.M, Hogan N, "Measurement of human ankle stiffness using the anklebot," *2007 IEEE 10th International Conference on Rehabilitation Robotics*, 2007.
- [28] A. Calanca, L. Capisani, and P. Fiorini, "Robust force control of series elastic actuators," *Actuators*, vol. 3, pp. 182–204, 2014
- [29] H. Amanda, E. Brian, and M. Goldfarb, "Variable cadence walking and ground adaptive standing with a powered ankle prosthesis," *IEEE TRANSACTIONS ON NEURAL SYSTEMS AND REHABILITATION ENGINEERING*, 2016.